

# Supramolecular photoswitch with white-light emission based on bridged bis(pillar[5]arene)s<sup>☆</sup>



G. Liu<sup>a, b</sup>, H. Zhang<sup>b, c</sup>, X. Xu<sup>a</sup>, Q. Zhou<sup>a</sup>, X. Dai<sup>a</sup>, L. Fan<sup>c</sup>, P. Mao<sup>c</sup>, Y. Liu<sup>a, \*</sup>

<sup>a</sup> College of Chemistry, State Key Laboratory of Elemento-Organic Chemistry, Nankai University, Tianjin 300071, PR China

<sup>b</sup> College of Science, Henan Agricultural University, Zhengzhou 450002, PR China

<sup>c</sup> College of Chemistry and Chemical Engineering, Henan University of Technology, Zhengzhou 450001, PR China

## ARTICLE INFO

### Article history:

Received 6 September 2021

Received in revised form

3 October 2021

Accepted 4 October 2021

Available online 5 November 2021

### Keywords:

Self-assembly

White light

Photocontrol

Light-harvesting

Host-guest complexation

## ABSTRACT

White light-emitting (WLE) switches have greatly promising and worthy applications in the field of controllable lighting, display, and sensing. Here, we unprecedentedly construct a photocontrollable light-harvesting supramolecular nanoassembly (**G/H@NiR**) with rarely switchable white light emission, which comprised oligo(phenylenevinylene)-bridged pillar[5]arenes (**H**), photochromic diarylethene (**G**), and Nile red (**NiR**), through host–guest complexation. In the nanosystem, color-tunable photoluminescence such as cyan, orange red, and especially white with chromaticity coordinates (0.33, 0.34) is achieved through altering the proportions of the energy donor (H in assembly **G/H**) and acceptor center (**NiR**). Importantly, **G**, acting as a modulator, can controllably change the energy-transfer (ET) pathway between **H** and **NiR**, when the **G/H@NiR** nanoassembly was exposed to distinct light, achieving reversible switching of multicolor photoluminescence including white-light emission. In addition, the designed intelligent supramolecular assembly **G/H@NiR** with captivating characteristics has extremely valuable application as erasable multicolor fluorescent inks to be filled in the groove of a three-dimensional model and further form a high-security-level chromatic anticounterfeiting quick response (QR) code, which can be completely hidden and revealed under stimulation of distinct light. Besides, the erasable fluorescent inks can also be used to record data information in mixed fiber film, which can be completely wiped off and rerecord by distinct light. The study provides a controllable supramolecular light-harvesting strategy (the photo-modulating ET pathway in the light-harvesting process) for developing photo-responsive intelligent photoluminescence materials, particularly photosensitive WLE materials, possessing potential applications in photosensitive lighting and display, multicolor imaging, light-manipulative data storage, and high-security-level anticounterfeiting.

© 2021 Elsevier Ltd. All rights reserved.

## 1. Introduction

The design and construction of color-tunable photoluminescence materials, especially white light-emitting (WLE) materials, have merited particular attention because of their attractive applications in lighting, display, and sensing [1–4]. Generally, WLE materials are produced by mixing blue and yellow fluorochromes, or via blending discrete red, green, and blue primary color luminescent dyes, as per the Commission Internationale de L'Eclairage (CIE) chromaticity diagram [5,6]. In recent years, supramolecular self-assembly has been handily used

to develop WLE systems through host–guest complexation-induced color-adjustable photoluminescence [7–10]. On the other hand, artificial light-harvesting systems based on fluorescence resonance energy transfer (FRET) with the color-tuning photoluminescence characteristic [11–14] provide an innovative platform for the fabrication of WLE materials. For developing the light-harvesting systems with high antenna effect, several strategies have been implemented so far, such as dendrimers [15,16], organogels [17,18], porphyrin arrays/assemblies [19,20], surface-cross-linked micelles [21], biopolymer assemblies [22,23], organic–inorganic hybrid materials [24,25], and macrocycle-based supramolecular assemblies [26–28]. More recently, artificial light-harvesting systems constructed through macrocycle-mediated supramolecular assembly gradually display a particular advantage in developing advanced WLE devices because diverse-color fluorochromes in this system can gather spontaneously through non-

<sup>☆</sup> This was dedicated to Sir Fraser Stoddart on the occasion of his 80th birthday.

\* Corresponding author.

E-mail address: [yuliu@nankai.edu.cn](mailto:yuliu@nankai.edu.cn) (Y. Liu).

covalent interaction to achieve FRET between them under certain conditions [29–32]. Nevertheless, most of artificial photo-harvesting systems with white-light emission reported so far were non-adjustable. It is well known that plants can alter their ET pathways to protect light-harvesting systems from damage when they are exposed to strong light [33]. This provided us guidance for the construction of the controllable artificial light-harvesting system. However, it is a huge challenge to build stimuli-switchable WLE materials based on the controllable light-harvesting platform.

We herein successfully developed an intelligently photo-responsive biomimetic light-harvesting system through non-covalent supramolecular assembling of oligo(phenylenevinylene)-bridged pillar[5]arenes (**H**), diarylethene-containing triazole butylcyanide branches (**G**), and Nile red (**NiR**). This system had several promising advantages shown as follows: (1) **H** held an excellent aggregation-induced emission (AIE) property in high concentration or insoluble solvent (high fraction of water) environment, and it is a good candidate for energy donor. (2) The introduction of the diarylethene unit to **G** endowed this system the photo-adjustable ability, which could effectively alter the ET pathway in this light-harvesting system. (3) Pillar[5]arenes and cyano-triazole branches were modified to **H** and **G**, respectively, leading to self-assembling of **G** and **H**. (4) **NiR**, a hydrophobic fluorochrome, could be loaded into the hydrophobic interlayer of the **G/H** nanoparticles and served as an energy acceptor center because of their energy matching. Therefore, the constructed supramolecular system not only possesses high ET efficiency, energy donor/acceptor ratio, and antenna effect but also is endowed with photo-tunable ability. To the best of our knowledge, this is the first time that a peculiar WLE molecular photoswitch is fabricated through a controllable supramolecular photo-harvesting strategy based on the photomodulation of the ET pathway (Scheme 1).

## 2. Results and discussion

### 2.1. Preparation of the host **H** and guest **G**

The novel host compound (**H**) and guest compound (**G**) were tactfully designed and successfully synthesized via several simple procedures (Scheme S1). The reaction of mono-bromine-modified P5 **1** with 4-hydroxy benzaldehyde in the presence of  $K_2CO_3$  obtained substance **2**. Subsequently, the mixture of **2** and 2,2'-(1,4-phenylene)diacetonitrile was refluxed in ethanol to give **H**. Alkyne **4** reacted with **5** under the catalysis of Cu(I) to prepare the guest **G**. Detailed synthetic procedures and characteristics of all new compounds were shown in the Supplementary Information.

### 2.2. Photoisomerization and photochromism of the guest compound **G**

In the view of the structural feature of **G**, its photoisomerization and photochromic properties were first evaluated. As displayed in Fig. 1a, the maximum absorption of the open form of **G** (OF-**G**) at 269 nm ( $\epsilon = 3.60 \times 10^4$  L/mol/cm) was gradually decreased on irradiation at 254 nm light, whereas two new absorptions at 373 nm ( $\epsilon = 8.20 \times 10^3$  L/mol/cm) and 570 nm ( $\epsilon = 9.80 \times 10^3$  L/mol/cm) emerged and increased, accompanied by the presence of an isosbestic point at 292 nm. Meanwhile, the color of the sample solution was changed from colorless to blue-violet (Fig. 1a, inset). The abovementioned phenomena were all attributed to photocyclization of OF-**G** to its closed-form (CF-**G**), as shown in Scheme 1. The photocyclization conversion was determined to be 85% by nuclear magnetic resonance (NMR) spectral examination of the irradiated sample (Fig. S1). Subsequently, photoirradiation of the resultant sample at >450 nm visible light triggered the UV-vis

absorption spectra, the color and NMR of the resultant sample to return to their original states (Fig. 1a and S2). These phenomena indicated the reversible photoisomerization of **G** between its open form and closed form as illustrated in Scheme 1. The photocyclization and photocycloreversion quantum yields were determined to be 0.54 and 0.019, respectively. Importantly, the photochromism of **G** manifested a good reversibility, and no apparent deterioration was observed even after seven times repeating cycles (Fig. 1b).

### 2.3. Construction of the photoresponsive binary supramolecular assembly **G/H**

As we all know, P5 and the neutral guests bearing two or three short alkyl chains with a triazole site and a cyano site at either end possessed strong binding ability with complex stability constant ( $K_S$ ) up to  $1.2 \times 10^4$  M<sup>-1</sup> in chloroform [34,35]. For examining the assembling behaviors of **G** and **H**, a series of experiments were then achieved. The NMR titration experiments were firstly carried out. From NMR titration spectroscopy (Fig. S3), the resonance for methylenes ( $H_{a-d}$ ) on **G** all showed an apparent upfield shift, and their integral areas maintained unchanged after continued addition of equivalent amounts of **H**, revealing a 1:1 host-guest binding stoichiometry. Their complex stability constant ( $K_S$ ) was determined to be  $1.47 \times 10^3$  M<sup>-1</sup> using the <sup>1</sup>H NMR single-point method [36,37]. More intuitively, the comparison of <sup>1</sup>H NMR spectroscopies of **H**, **G/H**, and **G** (Fig. 1c) manifested that the methylene groups between the cyano segment and triazole on **G** were apparently shifted upfield, indicating the segments were located in the cavity of P5 on **H**. In addition, further evidence provided by the two-dimensional rotating frame overhauser effect spectroscopy (ROSEY) spectrum (Fig. S4) indicated hydrogen-hydrogen correlation of the protons on methylene groups ( $H_{a-d}$ ) on **G** with the protons on methylene and phenyl groups of P5 on **H**, verifying the above-proposed assembling pattern. To further ascertain the assembling behaviors of **H** and **G**, diffusion-ordered spectroscopy (DOSY)-NMR spectra were subsequently performed to investigate which model (polymers, oligomers, or small-size supramolecular assemblies) was formed by **H** and **G**. As shown in Figs. S5–S7 and Table S1, the diffusion coefficient of **G/H** ( $3.48 \times 10^{-10}$  m<sup>2</sup>/s) was less than that of **H** ( $4.34 \times 10^{-10}$  m<sup>2</sup>/s) and **G** ( $8.72 \times 10^{-10}$  m<sup>2</sup>/s). As per the Stokes–Einstein equation, the average size of the assembly **G/H** was estimated to be 1.73 times sum of **H** and **G** by assuming the complexes as being hydrodynamically spherical [38,39], implying that **G/H** consisted of two small-size supramolecular assemblies, i.e. **G/H**[1 + 1] and **G/H**[2 + 2], as illuminated in Scheme 1. Furthermore, their high resolution mass spectrum (HR-MS) (Fig. S8) manifested the feasible structures of **G/H**[1 + 1] and **G/H**[2 + 2] (Scheme 1). In addition, relevant structural optimization and energy calculation were executed as well to support our viewpoints. As manifested in Fig. 2, the geometry-optimized structures of the two assemblies were consistent with the structures that we suspected (Scheme 1). In addition, the optimized geometries of their precursors and a series of relevant state functions (U, H, G,  $\Delta H$ ,  $\Delta U$ , and  $\Delta G$ ) also revealed that the proposed assembling patterns were relatively reasonable and the formation of **G/H**[2 + 2] had more favorable tendencies than that of **G/H**[1 + 1] because of relatively lower  $\Delta G$  of **G/H**[2 + 2] (Fig. S9 and Tables S2 and S3), which was consistent with composing proportion from DOSY results.

### 2.4. AIE of the binary supramolecular assembly

Afterward, the AIE property of **H** was investigated in consideration of introducing the diphenylethylene group [40,41]. As manifested in Fig. S10a, when water fraction ( $f_w$ ) of H<sub>2</sub>O-



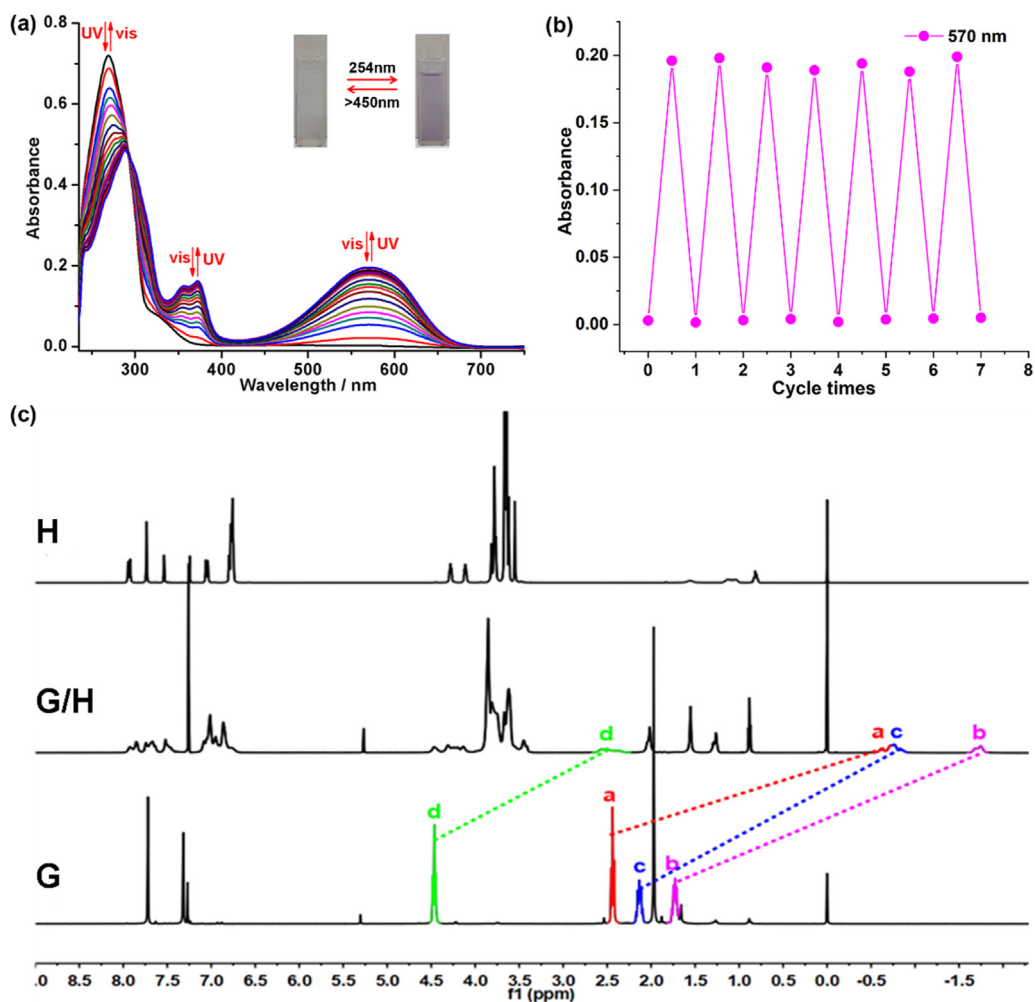


**Fig. 1.** (a) The absorption spectra and the alteration of photographs (inset) of G on irradiation at alternative 254 nm and >450 nm light,  $[G] = 2 \times 10^{-5}$  mol/L. (b) The variation of the absorbance of G at 570 nm on irradiation at alternative 254 nm and >450 nm light. (c) <sup>1</sup>H NMR (600 MHz, CDCl<sub>3</sub>, 25 °C) spectra of the host H, assembly G/H, and guest G.  $[H] = [G] = 5 \times 10^{-3}$  mol/L.

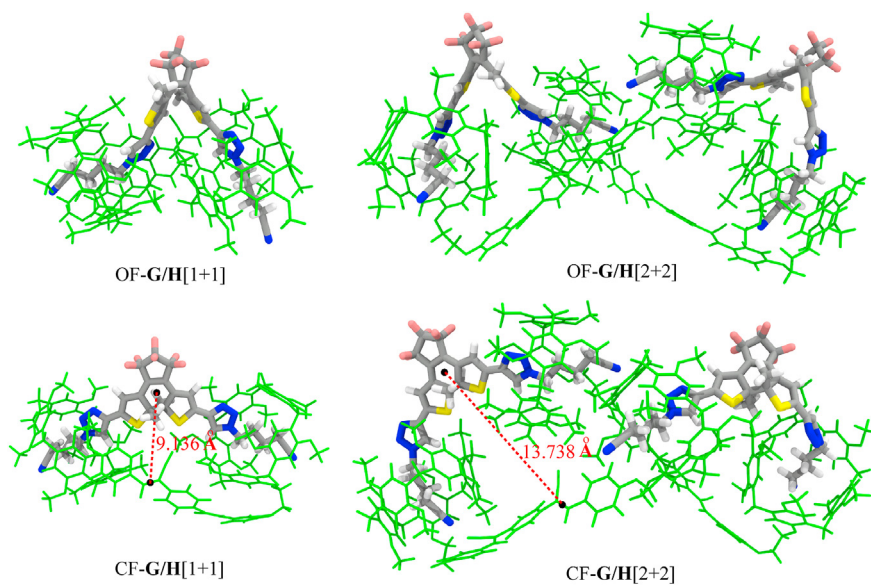


**Fig. 2.** Geometry-optimized structures of the supramolecular assemblies G/H[1 + 1] and G/H[2 + 2].

tetrahydrofuran (THF) mixed solvent was up to 80%, the fluorescence intensity of **H** was enhanced dramatically. Meanwhile, its emission maximum displayed a bathochromic shift by 76 nm by comparison of that in pure THF. Visually, gradual increase of undissolved water fraction turned on the Kelly fluorescence of **H** because of the formation of nanoaggregates, enabling naked-eye observation (Fig. S10c). These findings inspired us to further examine whether the supramolecular assembly **G/H** possessed the AIE property. To our delight, the assembly **G/H** also exhibited excellent AIE performance, and strong cyan fluorescence emerged with increase of water fraction to 90% (Fig. S10b and d). Discriminative fluorescence color and emission maximum (Fig. S11) were presented in **H** and **G/H** because of different aggregation degrees, implying the formation of two nanoaggregates. Furthermore, the UV-vis absorption spectra of **H** and **G/H** in  $f_w = 90\%$  THF-water mixed solution displayed an apparent bathochromic shift by 10 nm and 20 nm, respectively, and the absorption bands between 425 nm and 800 nm displayed an obvious upper shift, compared with that in pure THF solution (Fig. S12). These phenomena jointly implied that the nanoaggregates were formed and the **G/H** assembly exhibited tighter aggregation than **H** in  $f_w = 90\%$  THF-water mixed solution. The more intuitional proofs came from structural information of **G/H** given by transmission electron microscope (TEM), scanning electron microscope (SEM) and dynamic light scattering (DLS). The TEM image gave a distinct insight into the size and shape of the **G/H** assembly in  $f_w = 90\%$  H<sub>2</sub>O-THF mixed solvent. From the TEM image (Fig. 3a), we could find a lot of quasi-spherical nanostructures with an average diameter of 51 nm, indicating further aggregation of the assemblies into spherical nanoparticles, which was further confirmed by the SEM image (Fig. 3b). In addition, the hydrodynamic radius of **G/H** (ca. 99.94 nm) determined by DLS (Fig. 3c) was appreciably larger than the diameter observed by TEM because of the shrinking of nanoparticles on air-drying in the sample preparation for TEM [42]. Based on the morphological analyses, a plausible illustration of the spherical nanoparticle **G/H** was given in Scheme 1.

### 2.5. Multicolor and white light emission of light-harvesting ternary supramolecular assemblies

Inspired by the formation of the nanoaggregate **G/H** in inert solvent, we hypothesized that embedding another energy-matched

fluorescent dye into the supramolecular assemblies might fabricate a supramolecular light-harvesting system. It is feasible to implement that supramolecular assembly **G/H** loads some luminescent dyes as model substrates within the interior of the nanoparticles through hydrophobic effect and  $\pi-\pi$  interaction (Scheme 1). **NiR**, a fluorochrome with strong red emission in the hydrophobic environment, was chosen as a model substrate to construct a ternary supramolecular light-harvesting system because of the following advantages: (a) The absorption band of **NiR** mostly overlapped with the emission of OF-**G/H** in 90% water fraction of H<sub>2</sub>O-THF solvent (Fig. S13), which will be beneficial to the occurrence of the FRET process; (b) On account of no complexation of **NiR** with **H**, a spot of **NiR** could be loaded into the hydrophobic interlayer of the **G/H** assembly rather than encapsulated in the cavity of P5, where the **G/H** assembly could not dissociate. As manifested in Fig. 4a, when **G/H** was excited by 377 nm, the fluorescence intensity of **G/H** at 484 nm gradually declined; however, another emission at 590 nm (assigned to **NiR**) was progressively increased, with continuous addition of **NiR** to the assembly **G/H**. Visually, the strong cyan fluorescence was changed to orange red in the presence of a trace amount of **NiR** in this process, where the energy donor/acceptor (D/A) ratio is 100:3 (Fig. 4b). The fluorescence lifetimes ( $\tau$ ) of OF-**G/H** and OF-**G/H@NiR** were determined to be 6.69 ns ( $\lambda = 484$  nm) and 4.99 ns ( $\lambda = 590$  nm), respectively, when their excitation wavelengths were both 377 nm (Table S4 and Figs. S14 and S15). Meanwhile, their fluorescence quantum yields were determined to be 7.13% and 6.35% through the relative method (the reference compound was rhodamine B) on excitation at 365 nm (see Table S4 and the relevant calculation method in Supplementary Information). Very interestingly, when the D/A ratio was 160:3, strong white fluorescence appeared with the chromaticity coordinates (0.33, 0.34) in the abovementioned process (Fig. 4a–c), which would conduct as an excellent WLE material. The fluorescence quantum yield of OF-**G/H@NiR** with white-light emission was measured to be 6.36% through the same method as OF-**G/H** (Table S4). To confirm the occurrence of the abovementioned light-harvesting process, several control experiments were then conducted. Under the identical conditions, the same concentration of the samples containing free **NiR** (excitation at 377 nm or 543 nm) and **NiR** in the **G/H@NiR** assembly (excitation at 543 nm) in  $f_w = 90\%$  H<sub>2</sub>O-THF mixed solvent all exhibited a negligible fluorescence intensity in comparison with **G/H@NiR** on excitation at 377 nm (Figs. S16–S18). In

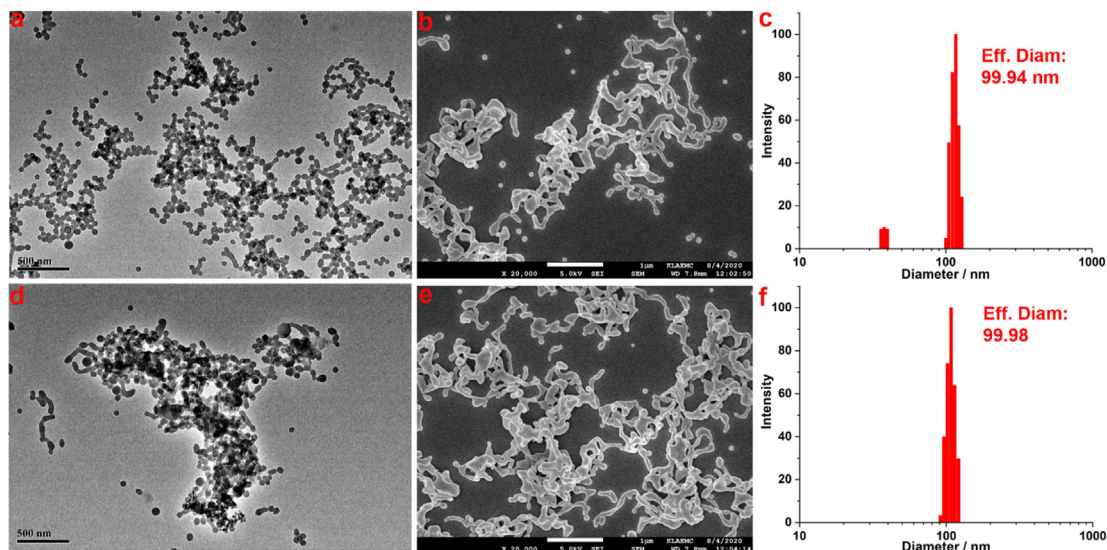


**Fig. 3.** (a) The TEM image of the **G/H** assembly; (b) The SEM image of the **G/H** assembly; (c) DLS data for **G/H** at 25 °C; (d) The TEM image of the **G/H@NiR** assembly; (e) The SEM image of the **G/H@NiR** assembly; (f) DLS data for **G/H@NiR** at 25 °C.

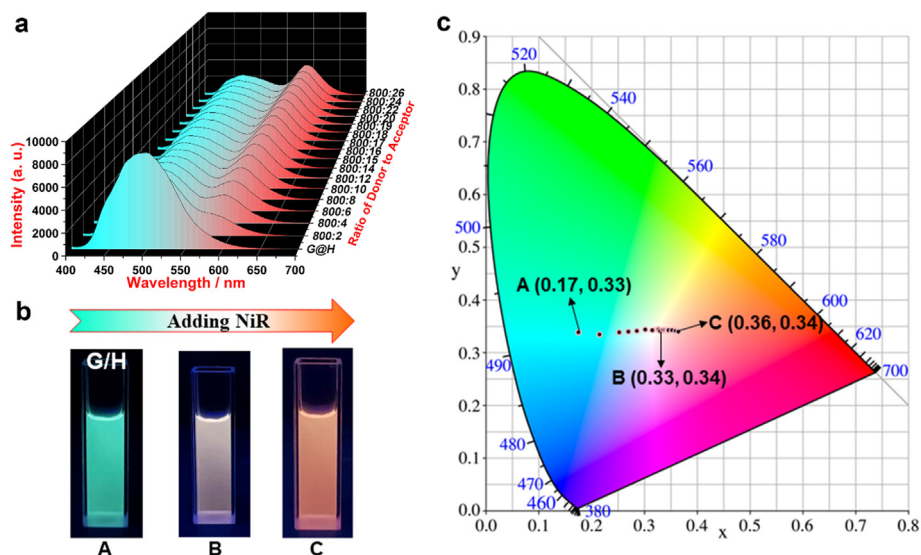


**Fig. 4.** (a) Fluorescence spectra of **G/H** ( $[G] = 1.0 \times 10^{-5}$  mol/L,  $[H] = 1.0 \times 10^{-5}$  mol/L) in  $f_w = 90\%$  THF-water mixed solution with sequential addition of **NiR**; The concentration of **NiR** was increased from 0 to  $3.0 \times 10^{-7}$  mol/L;  $\lambda_{\text{ex}} = 377$  nm; Slit = 5, 2.5. (b) Photographs of **G/H** and **G/H@NiR** under UV light (365 nm);  $[G] = 1.0 \times 10^{-5}$  mol/L,  $[H] = 1.0 \times 10^{-5}$  mol/L,  $[\text{NiR}] = 0$  mol/L (A),  $1.875 \times 10^{-7}$  mol/L (B), and  $3.0 \times 10^{-7}$  mol/L (C). (c) The 1931 CIE chromaticity coordinate changes from cyan (0.17, 0.33) to white (0.33, 0.34) and orange red (0.36, 0.34) with the addition of 0, 0.01875 eq (D/A = 160:3), and 0.03 eq (D/A = 100:3) of **NiR** to the **G/H** ( $[G] = [H] = 1.0 \times 10^{-5}$  mol/L) aqueous solution with  $\lambda_{\text{ex}} = 405$  nm, where X is the chromaticity coordinate that represents the proportion of red primary and Y is the chromaticity coordinate that represents the proportion of green primary.

consequence, we asserted that these small amounts of **NiR** were loaded in interior layers of the nanoparticles and light harvesting based on ET from **G/H** to **NiR** occurred in the ternary supramolecular nanosystem **G/H@NiR**. It is necessary to investigate the ET efficiency and antenna effect, which are two important factors in the artificial light-harvesting system. The  $\Phi_{\text{ET}}$  was determined approximately to be 69%, and the antenna effect was estimated to be 15.28 at a D/A ratio of 100:3 (see calculation details in Supporting Information). With the addition of **NiR**, there are no obvious changes in topological morphology and sizes of the **G/H** and **G/H@NiR** nanoaggregates through observation of TEM (Fig. 3d), SEM (Fig. 3e), and DLS (Fig. 3f) results of the ternary supramolecular assembly **G/H@NiR**, implying that **G/H** was simply loading toward **NiR** (as illuminated in Scheme 1). Furthermore, the nanoaggregates formed by only **H** could also load a spot of **NiR** to construct a light-harvesting system, but possessed lower ET efficiency (60%) and antenna effect (4.34) than that of **G/H@NiR** (Fig. S19).

## 2.6. Photosensitive multicolor and white light-emission switching of light-harvesting ternary supramolecular assemblies

By comprehensive analysis of photochromic and photoluminescence properties of the ternary supramolecular assembly **G/H@NiR**, it prospectively conducted as a photoresponsive artificial light-harvesting system. First, we studied photoswitchable photoluminescence behaviors of the binary assembly **G/H** in 90% water fraction of H<sub>2</sub>O-THF solution. It is well known that the fluorescence switching properties originate from good spectral overlap between the emission band of the fluorescence group and the absorption band of the colored photochromic unit [43,44]. To our delight, the emission spectrum of **H** possessed perfect overlap with the absorption spectrum of CF-**G** and had hardly any spectral overlap with OF-**G** that could not act as an energy receptor because of its high energy (Fig. S20). Owing to good photoisomerization performance of the guest **G**, the fluorescence of **G/H** at 484 nm was greatly quenched by 90% on irradiation at 254 nm UV light for just 10 s (Fig. 5a). Correspondingly, the strong cyan fluorescence became

almost invisible to the naked eyes (Fig. 5d). More quantitatively, the fluorescence quantum yield ( $\Phi_{\text{F}}$ ) was greatly decreased from 7.13% to 0.35% (Table S4). These observations were originated from photocyclization of OF-**G** to CF-**G** and occurrence of RET from **H** to non-luminous CF-**G** because the D/A distance as 9.136 Å or 13.738 Å (Fig. 2) was short enough within the range of the Förster radius ( $R_0 < 10$  nm) to facilitate the ET channel [45]. The ET efficiency ( $\Phi_{\text{ET}}$ ) from **H** to CF-**G** was calculated to be approximately 90% through tracking the change of fluorescence intensity at 484 nm (see calculation details in Supporting Information). To prove an important role in the photocontrolled ET process played by host-guest complexation, we selected the compound **R** (Scheme S1) without P5 instead of **H** to mix with **G** and further examined whether ET from **R** to **G** occurred. When the sample containing **G/R** was irradiated by 254 nm light, the fluorescence intensity was quenched by 60% (Fig. S21), which was apparently lower than ET efficiency of **G/H** (90%). The abovementioned phenomena implied that host-guest complexation closed the distance between the energy donor and acceptor. Subsequently, the quenched fluorescence of the **G/H** complex was completely recovered to its original level on continuous irradiation by the visible light (>490 nm) for 320 s, indicating inhibition of the RET process from **H** to **G**. This result was attributed to the reverse photoisomerization of **G** from CF to OF that had a high excitation energy mismatched with the emission energy of **H**. Importantly, the abovementioned photoinduced fluorescence switching process could be repeated for at least seven times without any recession (Fig. S22). Second, we investigated photo-responsive luminescence switching behaviors of the ternary supramolecular assembly **G/H@NiR** with orange red fluorescence (the D/A ratio was 100:3) under the encouragement of successful photoswitching fluorescence of the assembly **G/H**. Intriguingly, the fluorescence of **G/H@NiR** at 484 nm and 590 nm was strongly quenched by 82% and 98%, respectively, when it was irradiated by 254 nm UV light for 10 s (Fig. 5b). The total photo-triggered quenching rate of fluorescence emission and  $\Phi_{\text{ET}}$  in this process was estimated to be 90%, which was consistent with that of **G/H**, revealing that excitation energy of **H** in the **G/H@NiR** assembly should be transferred to non-luminous CF-**G**. Furthermore, the

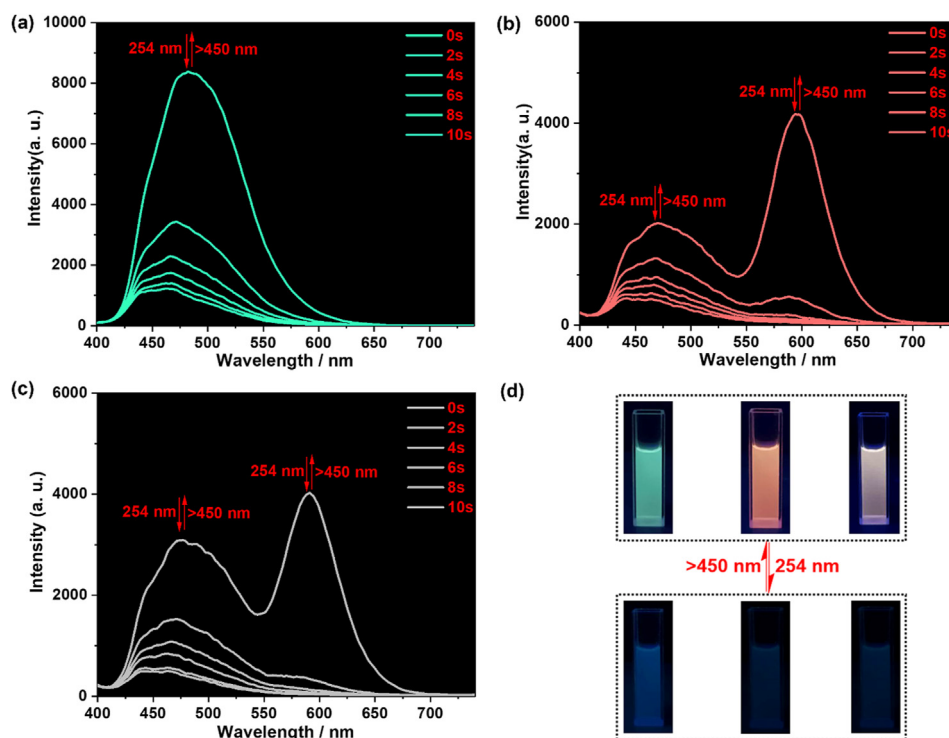


**Fig. 5.** The fluorescence spectra of **G/H** (a), **G/H@NiR** with the energy donor/acceptor ratio of 100:3 (b), and **G/H@NiR** with the energy donor/acceptor ratio of 160:3 (c) in  $f_w = 90\%$  THF-water mixed solution on irradiation at alternative 254 nm and >450 nm wavelength light; (d) Fluorescence photographs in the abovementioned process under UV light (365 nm);  $\lambda_{\text{ex}} = 377$  nm, Slit = 5, 2.5;  $[\text{G}] = 1.0 \times 10^{-5}$  mol/L,  $[\text{H}] = 1.0 \times 10^{-5}$  mol/L.

fluorescence of the **G/H@NiR** assembly at 590 nm was almost entirely quenched after irradiation at 254 nm light for 10 s, implying that the energy delivery from **H** to **NiR** was intercepted and then completely transferred to CF-**G** (as displayed in Scheme 1), probably because of the shorter D/A distance from **G** to **H** than that from **NiR** to **H**. Accordingly, the  $\Phi_F$  was decreased from 6.36% to 0.33% (Table S4), and the orange red fluorescence turned dark (Fig. 5d). Furthermore, another probable mechanism was that the excitation energy of **H** was delivered to **NiR** and subsequently transferred from **NiR** to CF-**G**, as shown in Fig. S23. However, to ascertain which mechanism was more convinced, we performed a control experiment. The concentration of **NiR** added was enhanced for convenient observation. As manifested in Fig. S24, the **G/H-NiR** mixture was irradiated for 10 s; the fluorescence intensity was slightly decreased. Therefore, we asserted the first probable mechanism (Scheme 1) should be dominant. Subsequently, when the resultant sample was irradiated by >450 nm visible light, the original fluorescence intensity and color were both restored, which was attributed to the excitation energy of **H** delivering to **NiR** again. The assembly also exhibited good fluorescence switching reversibility, and the proposed fluorescence switching mechanism in the abovementioned process was illuminated in Scheme 1. Finally, the **G/H@NiR** assembly (the D/A ratio was 160:3) with white-light emission was investigated on the photo-triggered luminescence switching behaviors. As discerned in Fig. 5c, to our excitement, the white fluorescence of the **G/H@NiR** assembly was reversibly switched 'on'/'off' on alternate irradiation at 254 nm and >450 nm light, accompanying by reversible alterations of fluorescence images (Fig. 5d). The present ternary supramolecular nanoassembly constructed by us was the first well-defined photosensitive white-light emitter, to the best of our knowledge. These observations were attributed to photochemical control of FRET from **H** to **NiR** through the interference of **G**, and the mechanism was completely identical with the **G/H@NiR** assembly (the D/A ratio was 100:3). Hence, these

ternary supramolecular nanosystems constructed by us were defined as distinguished photosensitive artificial light-harvesting systems based on the photo-modulating ET pathway.

### 2.7. High-security-level anticounterfeiting and data storage and confidentiality

With multicolor photoluminescence, photoresponsive performance, and good fatigue resistance in hand, the biomimetic light-harvesting nanomaterials fabricated by **G/H@NiR** could be applied in the multicolor fluorescent inks with erasable function for recording data information. As manifested in Fig. 6 (up), we fabricated a three-dimensional (3D) model of the QR code using 3D printing technology and filled the five color samples containing **H** (Kelly fluorescence), binary supramolecular assembly **G/H** (cyan fluorescence), ternary supramolecular assembly **G/H@NiR** with the diverse D/A ratio such as 160:3 (white fluorescence) and 100:3 (orange red fluorescence), and **NiR** (magenta fluorescence) in the 3D model. Then, under 365 nm light, a chromatic QR code emerged, and we could recognize the information from the QR code using our cellphone. Interestingly, when it was irradiated by 254 nm UV light for only 10 s, the QR code was destroyed and could not be observed completely, which was attributed to complete quenching in fluorescence of **G/H** and **G/H@NiR**. Crucially, the QR code could re-emerge with lossless again after irradiation of >450 nm visible light for 2 min. The aforementioned process could be repeated for many times without any recession, originating from good fatigue resistance of **G/H@NiR**. In addition, as shown in Fig. 6 (down), we drew a beautiful flower in mixed fiber film using the samples containing these ternary supramolecular assemblies with a diverse D/A ratio such as 400:1 (cyan fluorescence ink), 160:3 (white fluorescence ink), and 100:3 (orange red fluorescence ink), remaining likewise lifelike after drying under 365 nm light. Subsequently, the pattern could be completely erased on irradiation at UV (254 nm) light for

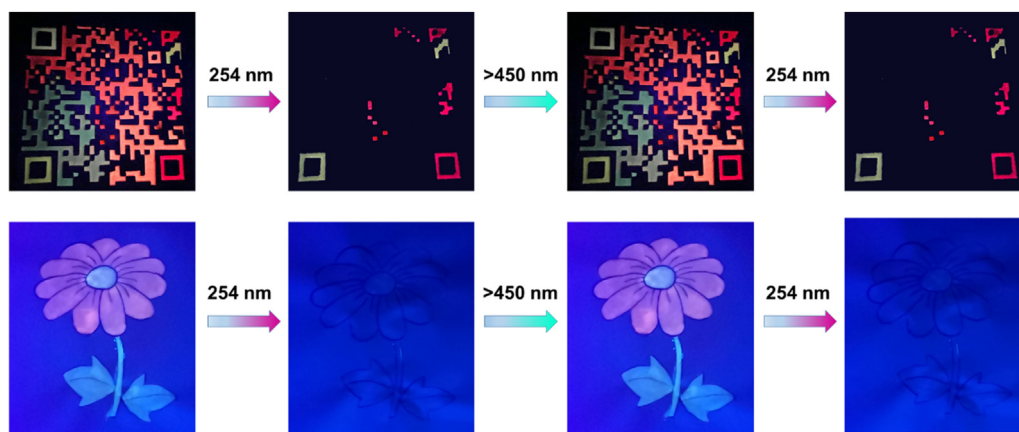


Fig. 6. The photo-switched chromatic fluorescent QR code and photo-manipulative data storage, anticounterfeiting, and data confidence.

only 10 s. Afterward, the fascinating pattern could reemerge with lossless again after irradiation of  $>450$  nm visible light for 2 min. The abovementioned recording-erasing behaviors could be conducted for lots of cycles without any recession as well.

### 3. Conclusion

In summary, we have fabricated unprecedentedly a rare photo-sensitive supramolecular light-harvesting WLE nanomaterial based on photoregulation of the ET pathway, which consisted of **H**, **G**, and **NiR**. **H** and **G** mainly formed a small-size supramolecular assembly **G/H**[2 + 2] as energy donors that further agglomerated into quasi-spherical nanoparticles in aqueous solution. The resultant nanoparticles could accommodate with energy acceptors (**NiR**) to form the biomimetic light-harvesting system **G/H@NiR** based on FRET. Along with addition of **NiR**, photoluminescence color of the light-harvesting system could be changed from cyan to orange red. Interestingly, white-light emission with the chromaticity coordinates (0.33, 0.34) emerged in the abovementioned process. Notably, in this system, the ET pathway from **H** to **NiR** could be reversibly intercepted and restored by **G** under stimulation of distinct lights. Thus, multicolor photoluminescence, particularly white-light emission formed by the system, could be further switched on/off on distinct light irradiation, which was greatly rare and intriguing. Crucially, the photo-responsive supramolecular smart materials based on the light-harvesting platform could act as erasable multicolor fluorescent inks to record the chromatic QR code and special pattern, which could be reversibly hidden and reemerge, presenting promising applications in data storage, diverse-color imaging, high-security-level anticounterfeiting, and WLE devices.

### CRedit author statement

**Guoxing Liu:** Conceptualization, Synthesis, Investigation, Methodology, Writing - original draft, Data curation. **Haifan Zhang:** Synthesis, Investigation, Methodology. **Xiufang Xu:** Theoretical calculations. **Qingyang Zhou:** Theoretical calculations. **Xiainyin Dai:** Investigation. **Lulu Fan:** Review. **Pu Mao:** Review. **Yu Liu:** Conceptualization, Review, Supervision.

### Declaration of competing interest

The authors declare that they have no known competing financial interests or personal relationships that could have appeared to influence the work reported in this article.

### Acknowledgments

The authors thank the National Natural Science Foundation of China (No. 21801063) and China Postdoctoral Science Foundation (No. 2018M642767) for financial support.

### Appendix A. Supplementary data

Supplementary data to this article can be found online at <https://doi.org/10.1016/j.mtchem.2021.100628>.

### References

- [1] B. Zhang, G. Tan, C.-S. Lam, B. Yao, C.-L. Ho, L. Liu, Z. Xie, W.-Y. Wong, J. Ding, L. Wang, High-efficiency single emissive layer white organic light-emitting diodes based on solution-processed dendritic host and new orange-emitting Iridium complex, *Adv. Mater.* 24 (2012) 1873–1877, <https://doi.org/10.1002/adma.2011104758>.
- [2] M. Chen, Y. Zhao, L. Yan, S. Yang, Y. Zhu, I. Murtaza, G. He, H. Meng, W. Huang, A unique blend of 2-fluorenyl-2-anthracene and 2-anthryl-2-anthracene showing white emission and high charge mobility, *Angew. Chem. Int. Ed.* 56 (2017) 722–727, <https://doi.org/10.1002/anie.201608131>.
- [3] M. Shang, C. Li, J. Lin, How to produce white light in a single-phase host? *Chem. Soc. Rev.* 43 (2014) 1372–1386, <https://doi.org/10.1039/C3CS60314H>.
- [4] M. Pan, W.-M. Liao, S.-Y. Yin, S.-S. Sun, C.-Y. Su, Single-phase white-light-emitting and photoluminescent color-tuning coordination assemblies, *Chem. Rev.* 118 (2018) 8889–8935, <https://doi.org/10.1021/acs.chemrev.8b00222>.
- [5] G.M. Farinola, R. Ragni, Electroluminescent materials for white organic light emitting diodes, *Chem. Soc. Rev.* 40 (2011) 3467–3482, <https://doi.org/10.1039/C0CS00204F>.
- [6] H.A. Höppe, Recent developments in the field of inorganic phosphors, *Angew. Chem. Int. Ed.* 48 (2009) 3572–3582, <https://doi.org/10.1002/anie.200804005>.
- [7] X.-L. Ni, S. Chen, Y. Yang, Z. Tao, Facile cucurbit[8]uril-based supramolecular approach to fabricate tunable luminescent materials in aqueous solution, *J. Am. Chem. Soc.* 138 (2016) 6177–6183, <https://doi.org/10.1021/jacs.6b01223>.
- [8] Q.W. Zhang, D. Li, X. Li, P.B. White, J. Mecnovic, X. Ma, H. Agren, R.J. Nolte, H. Tian, Multicolor photoluminescence including white-light emission by a single host-guest complex, *J. Am. Chem. Soc.* 138 (2016) 13541–13550, <https://doi.org/10.1021/jacs.6b04776>.
- [9] D. Li, F. Lu, J. Wang, W. Hu, X.-M. Cao, X. Ma, H. Tian, Amorphous metal-free room-temperature phosphorescent small molecules with multicolor photoluminescence via a host-guest and dual-emission strategy, *J. Am. Chem. Soc.* 140 (2018) 1916–1923, <https://doi.org/10.1021/jacs.7b12800>.
- [10] X.-Y. Lou, Y.-W. Yang, Aggregation-induced emission systems involving supramolecular assembly, *Aggregate* 1 (2020) 19–30, <https://doi.org/10.1002/agt2.1>.
- [11] H.-Q. Peng, L.-Y. Niu, Y.-Z. Chen, L.-Z. Wu, C.-H. Tung, Q.-Z. Yang, Biological applications of supramolecular assemblies designed for excitation energy transfer, *Chem. Rev.* 115 (2015) 7502–7542, <https://doi.org/10.1021/cr5007057>.
- [12] D. Li, J. Wang, X. Ma, White-light-emitting materials constructed from supramolecular approaches, *Adv. Opt. Mater.* 6 (2018) 1800273, <https://doi.org/10.1002/adom.201800273>.

- [13] Y. Chen, F. Huang, Z.-T. Li, Y. Liu, Controllable macrocyclic supramolecular assemblies in aqueous solution, *Sci. China Chem.* 61 (2018) 979–992, <https://doi.org/10.1007/s11426-018-9337-4>.
- [14] P. Li, Y. Chen, Y. Liu, Calixarene/pillararene-based supramolecular selective binding and molecular assembly, *Chin. Chem. Lett.* 30 (2019) 1190–1197, <https://doi.org/10.1016/j.ccl.2019.03.035>.
- [15] Y.H. Jeong, M. Son, H. Yoon, P. Kim, D.H. Lee, D. Kim, W.-D. Jang, Guest-induced photophysical property switching of artificial light-harvesting dendrimers, *Angew. Chem. Int. Ed.* 53 (2014) 6925–6928, <https://doi.org/10.1002/anie.201400835>.
- [16] J.-L. Wang, J. Yan, Z.-M. Tang, Q. Xiao, Y. Ma, J. Pei, Gradient shape-persistent  $\pi$ -conjugated dendrimers for light-harvesting: synthesis, photophysical properties, and energy funneling, *J. Am. Chem. Soc.* 130 (2008) 9952–9962, <https://doi.org/10.1021/ja803109r>.
- [17] A. Ajayaghosh, V.K. Praveen, C. Vijayakumar, Organogels as scaffolds for excitation energy transfer and light harvesting, *Chem. Soc. Rev.* 37 (2008) 109–122, <https://doi.org/10.1039/B704456A>.
- [18] P. Duan, N. Yanai, H. Nagatomi, N. Kimizuka, Photon upconversion in supramolecular gel matrixes: spontaneous accumulation of light-harvesting donor–acceptor arrays in nanofibers and acquired air stability, *J. Am. Chem. Soc.* 137 (2015) 1887–1894, <https://doi.org/10.1021/ja511061h>.
- [19] N. Aratani, D. Kim, A. Osuka, Discrete cyclic porphyrin arrays as artificial light-harvesting antenna, *Acc. Chem. Res.* 42 (2009) 1922–1934, <https://doi.org/10.1021/ar9001697>.
- [20] T.S. Balaban, Tailoring porphyrins and chlorins for self-assembly in biomimetic artificial antenna systems, *Acc. Chem. Res.* 38 (2005) 612–623, <https://doi.org/10.1021/ar040211z>.
- [21] H.-Q. Peng, Y.-Z. Chen, Y. Zhao, Q.-Z. Yang, L.-Z. Wu, C.-H. Tung, L.-P. Zhang, Q.-X. Tong, Artificial light-harvesting system based on multifunctional surface-cross-linked micelles, *Angew. Chem. Int. Ed.* 51 (2012) 2088–2092, <https://doi.org/10.1002/anie.201107723>.
- [22] C.V. Kumar, M.R. Duff, DNA-based supramolecular artificial light harvesting complexes, *J. Am. Chem. Soc.* 131 (2009) 16024–16026, <https://doi.org/10.1021/ja904551n>.
- [23] Q. Zou, K. Liu, M. Abbas, X. Yan, Peptide-modulated self-assembly of chromophores toward biomimetic light-harvesting nanoarchitectonics, *Adv. Mater.* 28 (2016) 1031–1043, <https://doi.org/10.1002/adma.201502454>.
- [24] K.V. Rao, K.K.R. Datta, M. Eswaramoorthy, S.J. George, Light-harvesting hybrid hydrogels: energy-transfer-induced amplified fluorescence in noncovalently assembled chromophore-organoclay composites, *Angew. Chem. Int. Ed.* 50 (2011) 1179–1184, <https://doi.org/10.1002/anie.201006270>.
- [25] I. Nabiev, A. Rakovich, A. Sukhanova, E. Lukashov, V. Zagidullin, V. Pachenko, Y.P. Rakovich, F.J. Donegan, A.B. Rubin, A.O. Govorov, Fluorescent quantum dots as artificial antennas for enhanced light harvesting and energy transfer to photosynthetic reaction centers, *Angew. Chem. Int. Ed.* 49 (2010) 7217–7221, <https://doi.org/10.1002/anie.201003067>.
- [26] J.-J. Li, Y. Chen, J. Yu, N. Cheng, Y. Liu, A supramolecular artificial light-harvesting system with an ultrahigh antenna effect, *Adv. Mater.* 29 (2017) 1701905, <https://doi.org/10.1002/adma.201701905>.
- [27] S. Guo, Y. Song, Y. He, X.-Y. Hu, L. Wang, Highly efficient artificial light-harvesting systems constructed in aqueous solution based on supramolecular self-assembly, *Angew. Chem. Int. Ed.* 57 (2018) 3163–3167, <https://doi.org/10.1002/anie.201800175>.
- [28] X.-M. Chen, Q. Cao, H.K. Bisoyi, M. Wang, H. Yang, Q. Li, An efficient near-infrared emissive artificial supramolecular light-harvesting system for imaging in the golgi apparatus, *Angew. Chem. Int. Ed.* 59 (2020) 10493–10497, <https://doi.org/10.1002/anie.202003427>.
- [29] Z. Xu, S. Peng, Y.-Y. Wang, J.-K. Zhang, A.I. Lazar, D.-S. Guo, Broad-spectrum tunable photoluminescent nanomaterials constructed from a modular light-harvesting platform based on macrocyclic amphiphiles, *Adv. Mater.* 28 (2016) 7666–7671, <https://doi.org/10.1002/adma.201601719>.
- [30] M. Hao, G. Sun, M. Zuo, Z. Xu, Y. Chen, X.-Y. Hu, L. Wang, A supramolecular artificial light-harvesting system with two-step sequential energy transfer for photochemical catalysis, *Angew. Chem. Int. Ed.* 59 (2020) 10095–10100, <https://doi.org/10.1002/anie.201912654>.
- [31] H. Wu, Y. Chen, X. Dai, P. Li, J.F. Stoddart, Y. Liu, In situ photoconversion of multicolor luminescence and pure white light emission based on carbon dot-supported supramolecular assembly, *J. Am. Chem. Soc.* 141 (2019) 6583–6591, <https://doi.org/10.1021/jacs.8b13675>.
- [32] J.-J. Li, H.-Y. Zhang, G. Liu, X. Dai, L. Chen, Y. Liu, Photocontrolled light-harvesting supramolecular assembly based on aggregation-induced excimer emission, *Adv. Opt. Mater.* 9 (2021) 2001702, <https://doi.org/10.1002/adom.202001702>.
- [33] J. Standfuss, A.C.T. van Scheltinga, M. Lamborghini, W. Kühlbrandt, Mechanisms of photoprotection and nonphotochemical quenching in pea light-harvesting complex at 2.5 Å resolution, *EMBO J.* 24 (2005) 919–928, <https://doi.org/10.1038/sj.emboj.7600585>.
- [34] C. Li, K. Han, J. Li, Y. Zhang, W. Chen, Y. Yu, X. Jia, Supramolecular polymers based on efficient pillar[5]arene-neutral guest motifs, *Chem. Eur. J.* 19 (2013) 11892–11897, <https://doi.org/10.1002/chem.201301022>.
- [35] X. Wang, H. Deng, J. Li, K. Zheng, X. Jia, C. Li, A neutral supramolecular hyperbranched polymer fabricated from an AB<sub>2</sub>-type copillar[5]arene, *Macromol. Rapid Commun.* 34 (2013) 1856–1862, <https://doi.org/10.1002/marc.201300731>.
- [36] L. Liu, N. Zhao, O.A. Scherman, Ionic liquids as novel guests for cucurbit[6]uril in neutral water, *Chem. Commun.* (2008) 1070–1072, <https://doi.org/10.1039/B716889F>.
- [37] W. Zhang, Y.-M. Zhang, S.-H. Li, Y.-L. Cui, J. Yu, Y. Liu, Tunable nanosupramolecular aggregates mediated by host–guest complexation, *Angew. Chem. Int. Ed.* 55 (2016) 11452–11456, <https://doi.org/10.1002/anie.201605420>.
- [38] R. Schmidt, M. Stolte, M. Grüne, F. Würthner, Hydrogen-bond-directed formation of supramolecular polymers incorporating head-to-tail oriented dipolar merocyanine dyes, *Macromolecules* 44 (2011) 3766–3776, <https://doi.org/10.1021/ma2004184>.
- [39] H.-G. Fu, H.-Y. Zhang, H.-Y. Zhang, Y. Liu, Photo-controlled chirality transfer and FRET effects based on pseudo[3]rotaxane, *Chem. Commun.* 55 (2019) 13462–13465, <https://doi.org/10.1039/C9CC06917H>.
- [40] J. Mei, N.L.C. Leung, R.T.K. Kwok, J.W.Y. Lam, B.Z. Tang, Aggregation-induced emission: together we shine, united we soar!, *Chem. Rev.* 115 (2015) 11718–11940, <https://doi.org/10.1021/acs.chemrev.5b00263>.
- [41] Z. Liu, X. Dai, Y. Sun, Y. Liu, Organic supramolecular aggregates based on water-soluble cyclodextrins and calixarenes, *Aggregate* 1 (2020) 31–44, <https://doi.org/10.1002/agt2.3>.
- [42] P. Huang, D. Wang, Y. Su, W. Huang, Y. Zhou, D. Cui, X. Zhu, D. Yan, Combination of small molecule prodrug and nanodrug delivery: amphiphilic drug–drug conjugate for cancer therapy, *J. Am. Chem. Soc.* 136 (2014) 11748–11756, <https://doi.org/10.1021/ja505212y>.
- [43] O. Kotova, R. Daly, C.M. dos Santos, M. Boese, P.E. Kruger, J.J. Boland, T. Gunnlaugsson, Europium-directed self-assembly of a luminescent supramolecular gel from a tripodal terpyridine-based ligand, *Angew. Chem. Int. Ed.* 51 (2012) 7208–7212, <https://doi.org/10.1002/anie.201201506>.
- [44] G. Bozoklu, C. Gateau, D. Imbert, J. Pécaut, K. Robeyns, Y. Filinchuk, M. Farah, M. Gilles, M. Mazzanti, Metal-controlled diastereoselective self-assembly and circularly polarized luminescence of a chiral heptanuclear europium wheel, *J. Am. Chem. Soc.* 134 (2012) 8372–8375, <https://doi.org/10.1021/ja3020814>.
- [45] J. Fan, M. Hu, P. Zhan, X. Peng, Energy transfer cassettes based on organic fluorophores: construction and applications in ratiometric sensing, *Chem. Soc. Rev.* 42 (2013) 29–43, <https://doi.org/10.1039/C2CS35273G>.